
[View Journal Online](#)
[View Article Online](#)

Synthesis, crystal structure, and antidiabetic property of hydrazine functionalized Schiff base: 1,2-Di(benzylidene)hydrazine

 Nilankar Diyali , Meena Chettri , Abhranil De  and Bhaskar Biswas *

Department of Chemistry, University of North Bengal, Darjeeling, 734013, India

 * Corresponding author at: Department of Chemistry, University of North Bengal, Darjeeling, 734013, India.
 e-mail: bhaskarbiswas@nbu.ac.in (B. Biswas).

RESEARCH ARTICLE

ABSTRACT



doi 10.5155/eurjchem.13.2.234-240.2265

Received: 10 March 2022

Received in revised form: 17 April 2022

Accepted: 27 April 2022

Published online: 30 June 2022

Printed: 30 June 2022

KEYWORDS

 Synthesis
 Hydrazine
 Schiff base
 Antidiabetic activity
 X-ray crystal structure
 Structural characterization

Hydrazine functionalized Schiff base, 1,2-di(benzylidene)hydrazine has been synthesized through a condensation between hydrazine and benzaldehyde under reflux, and structurally characterized. The crystal structure analysis reveals that the Schiff base crystallizes in an orthorhombic crystal system with the *Pbcn* space group. Crystal data for $C_{14}H_{12}N_2$: $a = 13.130(2)$ Å, $b = 11.801(2)$ Å, $c = 7.5649(16)$ Å, $V = 1172.1(4)$ Å³, $Z = 4$, $T = 298.0(2)$ K, $\mu(\text{MoK}\alpha) = 0.071$ mm⁻¹, $D_{\text{calc}} = 1.180$ g/cm³, 10252 reflections measured ($6.206^\circ \leq 2\theta \leq 65.352^\circ$), 2027 unique ($R_{\text{int}} = 0.0381$, $R_{\text{sigma}} = 0.0283$) which were used in all calculations. The final R_1 was 0.0627 ($I > 2\sigma(I)$) and wR_2 was 0.2462 (all data). It is evident that the imine protons are intramolecularly locked with the imine-N bond, and the phenyl rings exist in *anti* orientation with respect to the =N-N= bond adopting a nearly planar conformation. The Schiff base grows a one-dimensional framework in the crystalline phase through long-distant C-H... π interaction. Hirshfeld surface and energy framework analyses have also been performed to understand the supramolecular forces and their contributions meticulously. The hydrazine functionalized Schiff base showed an excellent antidiabetic activity through α -amylase inhibitory assay relative to a standard compound, acarbose under an identical condition.

 Cite this: *Eur. J. Chem.* 2022, 13(2), 234-240

 Journal website: www.eurjchem.com

1. Introduction

Hydrazine-containing compounds have gained the utmost importance as they serve as a fundamental unit in the areas of pharmaceuticals [1], agrochemicals [2], a precursor to polymerization catalysts [3,4], fuel [5,6], chemosensors [7], etc. The expanding research on the hydrazine-based molecule is evident from the world hydrazine market value which is US\$424 million in 2020 as per the report by Future Market Insight (FMI) and in 2021 the value surpassed US\$426 million [8]. On the verge of the development of efficient hydrazine-based materials, many functionalizations have been achieved [9-12]. The functionalization of hydrazine improves the efficiency of the materials and may create new properties in it. Among various functionalizations, one with Schiff base is trending due to the diverse properties of Schiff base including antibacterial [13,14], antifungal [15-17], antioxidant [18-20], antiviral [21], antitumor [22], anti-inflammatory [23,24], biomimics [25], luminescence [26] and catalytic activity [27-29]. A brief literature survey shows that Biswas *et al.* has successfully designed a Schiff base functionalized with hydrazine and employed it for the synthesis of nanoaggregates that showed blue emission properties [30]. Additionally, Roy *et al.* developed an analogue of hydrazine-functionalized Schiff base and used it for cascade sensing for fluoride and bisulphate [7]. On the other hand, the tremendous

rise in the field of pharmaceutical and medicinal chemistry has drawn the attention of researchers toward the formulation of efficient drugs even for the treatment of diseases as complex as diabetes mellitus. Diabetes mellitus, one of the global health issues, is due to irregular insulin production that can lead to a series of other diseases. Recently, functionalized Schiff bases are found to be a promising candidate in this field [31]. In various studies conducted to investigate insulin-mimetic properties, hydrazine derivatives of Schiff base have some interesting results, for example, Szklarzewick's group showed the antidiabetic potentiality of a Schiff base [32]. In this context, we report the synthesis, crystal structure, Hirshfeld surface, and energy framework analysis of novel hydrazine functionalized Schiff base. We have also evaluated the antidiabetic activity of the prepared Schiff base by α -amylase inhibitory assay.

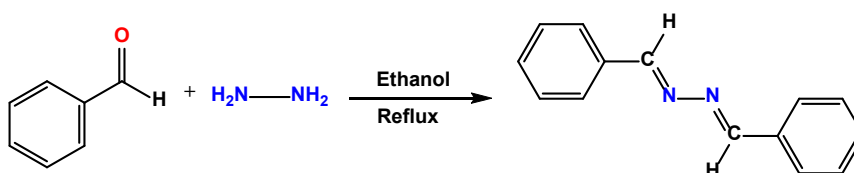
2. Experimental

2.1. Instrumentations

The percentage contribution of the elements of the Schiff base was determined on a Perkin Elmer 2400 CHN Elemental Analyzer.

Table 1. Crystal data and structure refinement for the Schiff base.

Empirical formula	C ₁₄ H ₁₂ N ₂
Formula weight	208.26
Temperature (K)	298.0(2)
Crystal system	Orthorhombic
Space group	Pbcn
<i>a</i> , (Å)	13.130(2)
<i>b</i> , (Å)	11.801(2)
<i>c</i> , (Å)	7.5649(16)
Volume (Å ³)	1172.1(4)
<i>Z</i>	4
ρ_{calc} (g/cm ³)	1.180
μ (mm ⁻¹)	0.071
F(000)	440.0
Crystal size (mm ³)	0.5 × 0.14 × 0.09
Radiation	MoK α (λ = 0.71073)
2 θ range for data collection (°)	6.206 to 65.352
Index ranges	-9 ≤ <i>h</i> ≤ 18, -15 ≤ <i>k</i> ≤ 15, -10 ≤ <i>l</i> ≤ 8
Reflections collected	10252
Independent reflections	2027 [R _{int} = 0.0381, R _{sigma} = 0.0283]
Data/restraints/parameters	2027/0/73
Goodness-of-fit on F ²	1.007
Final R indexes [I ≥ 2 σ (I)]	R ₁ = 0.0627, wR ₂ = 0.1795
Final R indexes [all data]	R ₁ = 0.1270, wR ₂ = 0.2462
Largest diff. peak/hole (e.Å ⁻³)	0.15/-0.18

**Scheme 1.** Synthetic procedure of the compound.

An FTIR-8400S Shimadzu spectrophotometer was employed to record the infrared spectrum (KBr) in the range of 400-3600 cm⁻¹. The UV-Vis spectrum of the synthetic compound was measured on a Hitachi U2910 spectrometer.

2.2. Synthesis

High purity hydrazine monohydrate (Merck, India) and benzaldehyde (SRL, India) were obtained from commercial sources and used as received. All the reagents and solvents were of analytical grade. Hydrazine monohydrate (0.032 g, 1 mM) was refluxed with benzaldehyde (0.212 g, 2 mM) in a 1:2 stoichiometric ratio in 30 mL of ethanol. The reaction mixture was filtered and upon slow cooling of the reaction, the solution produced suitable colourless crystals. The crystals were collected and washed with *n*-hexane. Further, the crystals were dried and kept over silica gel indicator for subsequent uses (Scheme 1). Yield: 0.188 g (~90%). Anal. calcd. for C₁₄H₁₂N₂: C, 80.74; H, 5.81; N, 13.45. Found: C, 80.71; H, 5.85; N, 13.52. IR (KBr, ν , cm⁻¹): 1614, 1587 (C=N). UV-Vis (λ_{max} , nm): 227, 254.

2.3. Single crystal X-ray diffraction study

Single crystal X-ray diffraction data were recorded with a Rigaku XtaLABmini diffractometer on a Mercury375R (2×2 bin mode) CCD detector using a graphite monochromated MoK α radiation (λ = 0.71075 Å) at 293(2) K using ω scans. The data were reduced and the space group was determined by Crystalclear suite [33] and OLEX2, respectively [34]. The structure was resolved and refined by full-matrix least-squares procedures with SHELXL-97 [35] and OLEX2 suite [34] (Table 1).

2.4. Hirshfeld surface and energy framework analysis

Hirshfeld surface and 2D fingerprint plots were generated by Crystal Explorer 17.5 program [36,37]. The energy framework analysis of the synthetic Schiff base was pursued

with Crystal Explorer software with B3LYP/6-31G(d,p) basis sets using TONTO software for the cluster environment of 3.8 Å surrounding a particular molecule of interest [38]. The total interaction energy is articulated as $E_{\text{tot}} = k_{\text{ele}}E'_{\text{ele}} + k_{\text{pol}}E'_{\text{pol}} + k_{\text{disp}}E'_{\text{disp}} + k_{\text{rep}}E'_{\text{rep}}$, where the *k* values belong to the scale factors for benchmarked energy models. E'_{ele} represents the electrostatic energy, E'_{pol} represents the polarization energy, E'_{disp} represents the dispersion energy, and E'_{rep} represents the repulsive energy.

2.5. Antidiabetic study

The antidiabetic study of the synthetic Schiff base was carried out following a review of the literature [39]. The reaction mixture was prepared by adding 25 mL of sample solution (100-400 $\mu\text{g/mL}$), 50 μL of α -amylase (10 $\mu\text{g/mL}$) solution in phosphate buffer (pH = 6.9) and 50 μL of starch solution (0.05%). The reaction was stopped by adding 25 μL of 1 M HCl followed by adding up 100 mL of iodine-potassium iodide solution. The solution mixture was incubated for 10 min at 37 °C followed by measuring the absorbance at 630 nm. Acarbose was used as a positive control. The following formula was used to calculate the α -amylase inhibitory activity.

$$\% \text{ Inhibitory activity} = [(A_0 - A_1)/A_0] \times 100 \quad (1)$$

A_0 = Absorbance of the control and A_1 = Absorbance of the test samples. After determining the α -amylase inhibitory activity of the different concentrations, the IC₅₀ values were determined for the acarbose and samples.

3. Results and discussion

3.1. Synthesis

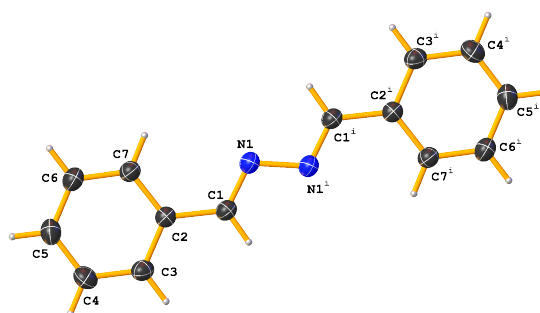
The hydrazine functionalized compound was synthesized by condensing hydrazine with benzaldehyde under reflux in ethanol.

Table 2. Bond distances, bond angles and torsion angles for the Schiff base.

Bond distances										
Atom	Atom	Length (Å)	Atom	Atom	Length (Å)					
N1	N1 ⁱ	1.419(3)	C7	C6	1.376(3)					
N1	C1	1.265(2)	C3	C4	1.382(3)					
C2	C1	1.464(2)	C6	C5	1.368(3)					
C2	C7	1.388(2)	C4	C5	1.375(3)					
C2	C3	1.391(2)								
Bond angles										
Atom	Atom	Atom	Angle (°)	Atom	Atom	Atom	Angle (°)			
C1	N1	N1 ⁱ	112.93(17)	C6	C7	C2	120.22(18)			
C7	C2	C1	121.72(16)	C4	C3	C2	120.58(18)			
C7	C2	C3	118.58(17)	C5	C6	C7	120.83(18)			
C3	C2	C1	119.69(15)	C5	C4	C3	119.90(19)			
N1	C1	C2	122.51(16)	C6	C5	C4	119.9(2)			
Torsion angles										
Atom	Atom	Atom	Atom	Angle (°)	Atom	Atom	Atom	Atom	Angle (°)	
N1 ⁱ	N1	C1	C2	179.43(14)	C1	C2	C7	C6	-179.07(17)	
C1	N1	N1 ⁱ	C1 ⁱ	180.00(15)	C3	C2	C7	C6	-0.4(2)	
N1	C1	C2	C3	178.99(16)	C2	C3	C4	C5	0.6(3)	
N1	C1	C2	C7	-2.3(3)	C3	C4	C5	C6	-0.9(3)	
C1	C2	C3	C4	178.79(17)	C4	C5	C6	C7	0.6(3)	
C7	C2	C3	C4	0.0(3)	C5	C6	C7	C2	0.1(3)	

ⁱ Symmetry code: 1-x, 1-y, 1-z.**Table 3.** Geometrical parameters of C-H... π interactions (Å, °) are involved in the supramolecular construction. D = Donor, A = Acceptor (Å, °).

D-H...A (Å)	d(D-H)	d(H...A)	d(D...A)	\angle D-H...A	Symmetry
C(3)-H(3)...Cg(1)	0.95	2.96	3.91	143	3/2-x, 1/2-y, -1/2+z

**Figure 1.** ORTEP diagram of the Schiff base (1) *i*: 1-x, 1-y, 1-z.

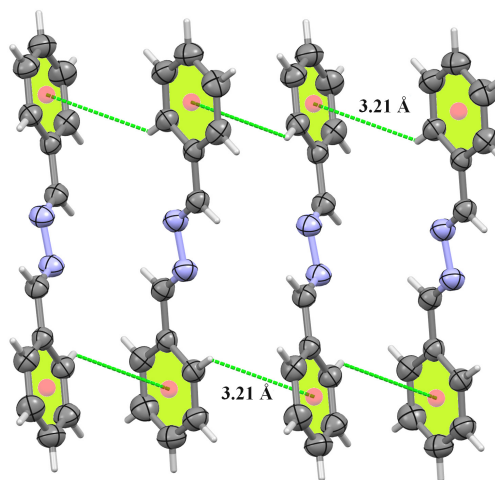
Upon slow cooling of the hot ethanolic reaction mixture, suitable crystals were obtained. The crystals were diffracted with the X-ray diffraction technique. The composition was established by spectral analysis and X-ray crystallography. The synthetic scheme is given by Scheme 1.

3.2. Crystal structure and supramolecular interactions

The crystal structure analysis of the Schiff base reveals that the synthetic compound exists in an orthorhombic crystal lattice with the *Pbcn* space group. An ORTEP diagram of the asymmetric unit is shown in Figure 1. The crystallographic refinement parameters for the Schiff base are presented in Table 1 and the bond angles and distances are presented in Table 2.

The crystal structure analysis shows that the hydrazine functionalized Schiff bases exist in a locked state with strong intramolecular H-bonded interactions and adopt *anti*-conformation (Figure 1). In the asymmetric unit, the azomethine bond distance between C1 and N1 atoms was found to be 1.265(2) Å while the N1-N1ⁱ bond distance value was marked as 1.419(3) Å. The bond distance values corroborate a pure double and single bond character for C1-N1 and N1-N1ⁱ bonds, respectively (Table 2) [40]. Further, the bond angles C2-C1-N1 and C1-N1-N1ⁱ (*i*: 1-x, 1-y, 1-z) are estimated as 122.51(16) and 112.93(17)° attributing to the planarity of the asymmetric unit in the crystalline phase [41]. The measurement of torsion angles further supports the planar geometry of the molecule (Table 2). The role of supramolecular interactions is also assessed for the construction of a long-range

architecture. It is revealed that the Schiff base functionalized with hydrazine develops a one-dimensional supramolecular framework through long-distant C-H... π interactions [42] (Figure 2, Table 3). In the formation of the long-range supramolecular architecture, the azomethine-N of the synthetic Schiff base involves very little interaction in the intermolecular hydrogen bonding as it is intramolecularly locked with imine-proton while the phenyl-H contributes to a great extent through C-H... π interactions.

**Figure 2.** Stacking of asymmetric units through weak C-H... π interactions.

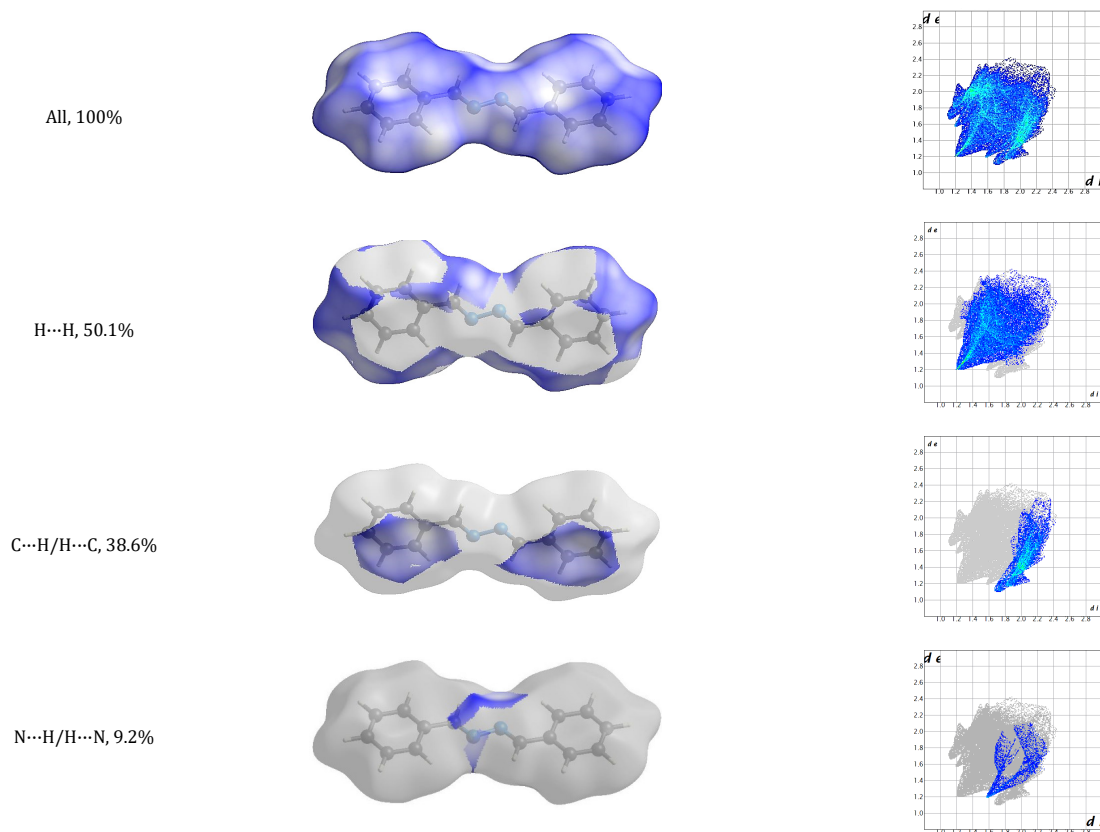


Figure 3. 2-Dimensional fingerprint plot of the main intermolecular interactions in the crystal structure of the title compound.

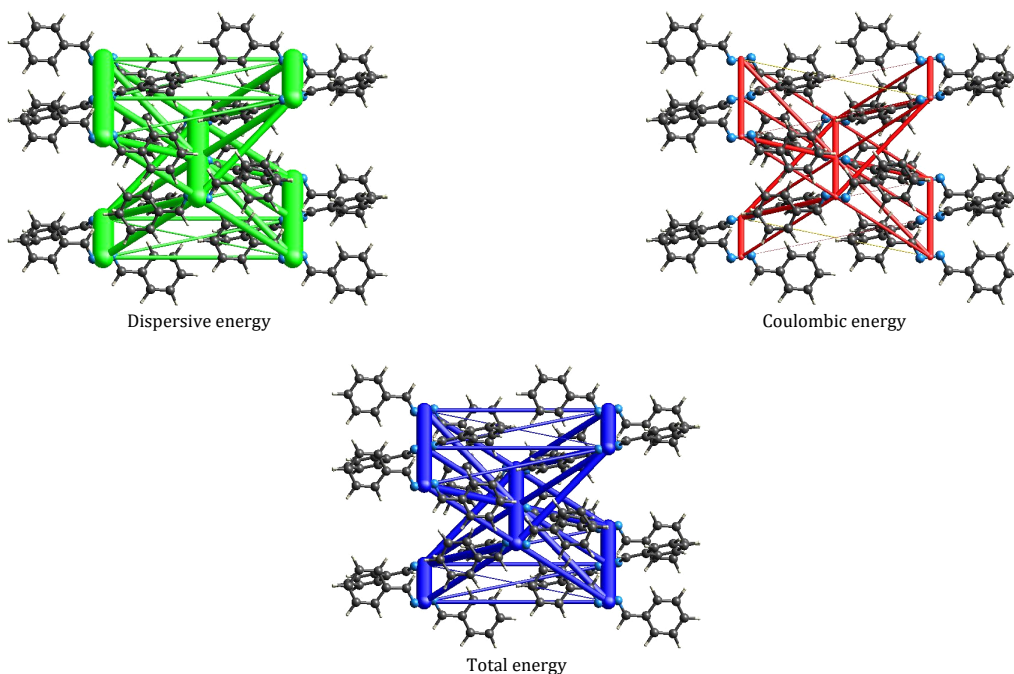
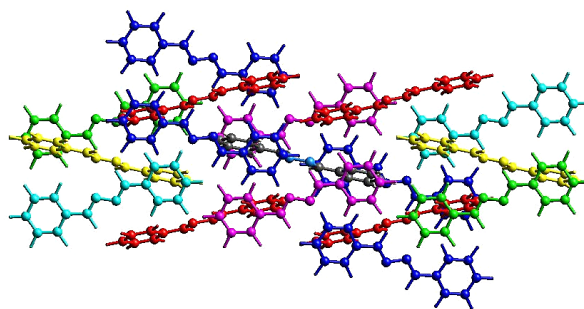


Figure 4. Energy framework diagrams for title compound, showing their respective type of energies.

The role of C-H \cdots π interaction in the supramolecular framework was also confirmed by Hirshfeld surface analysis (Figure 3). It is observed that N \cdots H hydrogen bonding only makes 9.2% and C-H \cdots π interactions cover 22.1% of the total surface area in the long-range architecture for the synthetic Schiff base. Other non-classical interactions were not significant as evidenced by the Hirshfeld 2D fingerprint plots (Figure 3).

Further, the energy framework analysis suggests that the dispersive force (-92.0 kJ/mol) made a significant contribution to the overall framework energy diagram of the Schiff base (Figure 4). C-H \cdots π interactions remain the origin to cause the dispersive force in the supramolecular framework (Table 4).

Table 4. Energy framework detail of interaction with symmetry operations (symop) and distances between molecular centroids (R).

Color	N	Symop	R	Electron density	E_{ele}	E_{pol}	E_{dis}	E_{rep}	E_{tot}
Red	4	$x+1/2, -y+1/2, -z$	8.83	B3LYP/6-31G(d,p)	-2.7	-0.8	-15.6	8.9	-11.5
Yellow	2	x, y, z	13.13	B3LYP/6-31G(d,p)	0.2	-0.2	-8.8	0.0	-7.6
Green	2	$-x, y, -z+1/2$	13.66	B3LYP/6-31G(d,p)	-0.4	-0.2	-6.0	0.0	-5.8
Cyan	2	$-x, y, -z+1/2$	13.66	B3LYP/6-31G(d,p)	0.8	-0.1	-3.2	0.0	-2.0
Purple	4	$-x+1/2, -y+1/2, -z+1/2$	9.60	B3LYP/6-31G(d,p)	-3.8	-0.5	-15.3	6.2	-13.9
Pink	2	$-x, y, -z+1/2$	3.78	B3LYP/6-31G(d,p)	-5.8	-2.0	-43.1	28.3	-27.6
Total					-11.7	-3.8	-92.0	43.4	-68.4

* Interaction energies (kJ/mol), R is the distance between molecular centroids (mean atomic position) in Å, Total energies, only reported for two benchmarked energy models, are the sum of the four energy components.

Table 5. α -Amylase inhibitory activity of acarbose and Schiff base.

Sample	Concentration ($\mu\text{g/mL}$)	% Inhibition
Acarbose	100	79.98 \pm 2.29
	200	83.87 \pm 0.29
	300	85.78 \pm 0.37
	400	94.24 \pm 1.74
Schiff base	100	66.98 \pm 1.37
	200	70.40 \pm 0.45
	300	78.70 \pm 2.29
	400	85.12 \pm 0.44

3.3. Antidiabetic study

The antidiabetic activity of the synthetic compound was evaluated in a dose-dependent manner. For the treatment of diabetes mellitus, inhibitory action on carbohydrate digesting enzymes like α -amylase and α -glucosidase is preliminary. Conventionally used starch iodine method for α -amylase inhibitory activity making use of the synthetic Schiff base has some intriguing results. The dose-dependent α -amylase inhibition assay (Table 5) reveals that on an average \sim 75% inhibition activity is found for the synthetic Schiff base. Acarbose is used as a standard antidiabetic agent which showed a slightly higher \sim 86% inhibition activity [43-45]. The IC_{50} values for the synthetic Schiff base and acarbose are also determined to be 74.67 and 62.05 $\mu\text{g/mL}$, respectively. The IC_{50} values are comparable and express the potential capacity of the synthetic Schiff base to turn out as an excellent anti-diabetic agent.

4. Conclusions

We have reported a straightforward synthesis of a hydrazine-functionalized Schiff base and its structural characterization with spectroscopy and X-ray crystallography. Crystal structure analysis suggested that the Schiff base adopts a nearly planar structure with an *anti*-orientation of phenyl rings with respect to =N-N= linkage. More interestingly, the imine-Hs are locked with the N-atom of the azomethine group attributing a hindrance to the excited state electron transfer phenomenon. Moreover, the asymmetric unit of the Schiff base displays the formation of a 1D supramolecular framework through long-distant C-H \cdots π interactions in crystallizing phase.

The significant contribution of C-H \cdots π interactions for the long-range crystalline framework of the synthetic Schiff base was evidenced by the 22.1% coverage of the Hirshfeld surface and the estimated dispersive force, -92.0 kJ/mol to the overall energy of the Schiff base (-68.4 kJ/mol). The synthetic Schiff-based showed an excellent α -amylase inhibitory activity. The comparable IC_{50} value of the Schiff base relative to the standard antidiabetic agent, acarbose holds a great promise for designing a cost-effective antidiabetic agent.

Supporting information

CCDC-2157622 contains the supplementary crystallographic data for this paper. These data can be obtained free of charge via <https://www.ccdc.cam.ac.uk/structures/>, by e-mailing data_request@ccdc.cam.ac.uk, or by contacting The Cambridge Crystallographic Data Centre, 12 Union Road, Cambridge CB2 1EZ, UK; fax: +44(0)1223-336033.

Disclosure statement

Conflict of interest: The authors declare that they have no conflict of interest. Ethical approval: All ethical guidelines have adhered to. Sample availability: Samples of the compounds are available from the author.

CRedit authorship contribution statement

Conceptualization: Bhaskar Biswas Methodology: Nilankar Diyali, Meena Chettri Software: Nilankar Diyali; Validation: Bhaskar Biswas Formal Analysis: Nilankar Diyali, Meena Chettri, Abhramil De Investigation: Bhaskar Biswas, Nilankar Diyali, Meena Chettri Resources: Abhramil De, Bhaskar Biswas; Data Curation: Bhaskar Biswas Writing - Original Draft: Bhaskar Biswas Writing - Review and Editing: Bhaskar Biswas; Visualization: Bhaskar Biswas.

ORCID  and Email 

Nilankar Diyali

 nilankardiyali02@gmail.com <https://orcid.org/0000-0002-1064-8308>

Meena Chettri

 chettrimeena78@gmail.com <https://orcid.org/0000-0003-2821-8880>

Abhranil De

 abhbranilde@gmail.com <https://orcid.org/0000-0002-6131-2548>

Bhaskar Biswas

 bhaskarbiswas@nbu.ac.in icbbiswas@gmail.com <https://orcid.org/0000-0002-5447-9729>

References

- Jucker, E. Recent pharmaceutical research on hydrazine derivatives. *Pure Appl. Chem.* **1963**, *6*, 409–434.
- Toki, T.; Koyanagi, T.; Yoshida, K.; Yamamoto, K.; Morita, M. Hydrazine compounds useful as pesticides. 5304657, April 19, 1994.
- Butufe, O.; Mazare, M.; Deaconescu, I.; Rolea, G.; Pascu, C.; Nicolescu, I. V. Polymer Catalysts. *J. Macromol. Sci. - Chem.* **1985**, *22*, 889–895.
- Parravano, G. Polymerization induced by catalytic decomposition of hydrazine at palladium surfaces. *J. Am. Chem. Soc.* **1950**, *72*, 3856–3860.
- Evans, D. D.; Price, T. W. The status of monopropellant hydrazine technology. *JPL Technical Report* **1968**, 32-722. <https://ntrs.nasa.gov/api/citations/19680006875/downloads/19680006875.pdf> (accessed April 10, 2022).
- Clark, J. D. *Ignition!: An informal history of liquid rocket propellants*; Rutgers University Press: New Brunswick, NJ, 2018.
- Roy, S.; Paul, P.; Karar, M.; Joshi, M.; Paul, S.; Choudhury, A. R.; Biswas, B. Cascade detection of fluoride and bisulphate ions by newly developed hydrazine functionalised Schiff bases. *J. Mol. Liq.* **2021**, *326*, 115293.
- Future Market Insights Global; Consulting Pvt. Ltd. Hydrazine Hydrate Market to be worth US\$ 683.1 Million by the year 2030 - Comprehensive Research Report by FMI. <https://finance.yahoo.com/news/hydrazine-hydrate-market-worth-us-180000622.html> (accessed April 10, 2022).
- Costoyas, A.; Ramos, J.; Forcada, J. Hydrazine-functionalized latexes: Hydrazine-functionalized latexes. *J. Polym. Sci. A Polym. Chem.* **2009**, *47*, 6201–6213.
- Huang, G.; Sun, Z.; Qin, H.; Zhao, L.; Xiong, Z.; Peng, X.; Ou, J.; Zou, H. Preparation of hydrazine functionalized polymer brushes hybrid magnetic nanoparticles for highly specific enrichment of glycopeptides. *Analyst* **2014**, *139*, 2199–2206.
- Afzal, S.; Al-Rashida, M.; Hameed, A.; Pelletier, J.; Sévigny, J.; Iqbal, J. Functionalized oxindolin hydrazine carbothioamide derivatives as highly potent inhibitors of nucleoside triphosphate diphospho hydrolases. *Front. Pharmacol.* **2020**, *11*, 585876.
- Jha, A. K.; Sarita; Easwar, S. Unsymmetrical N,N'-functionalization of hydrazine by insertion into Morita-Baylis-Hillman ketones. *Tetrahedron Lett.* **2021**, *69*, 152971.
- Sani, U.; Dailami, S. A. Synthesis, characterization, antimicrobial activity and antioxidant studies of metal (II) complexes of Schiff base derived from 2 - hydroxy - 1- naphthaldehyde and hydrazine mono hydrate. *ChemSearch Journal* **2015**, *6*, 35–41.
- Ceramella, J.; Iacopetta, D.; Catalano, A.; Cirillo, F.; Lappano, R.; Sinicropi, M. S. A review on the antimicrobial activity of Schiff bases: Data collection and recent studies. *Antibiotics (Basel)* **2022**, *11*, 191.
- Manimohan, M.; Pugalmani, S.; Sithique, M. A. Biologically active novel N, N, O donor tridentate water soluble hydrazide based O-carboxymethyl chitosan Schiff base Cu (II) metal complexes: Synthesis and characterisation. *Int. J. Biol. Macromol.* **2019**, *136*, 738–754.
- da Silva, C. M.; da Silva, D. L.; Modolo, L. V.; Alves, R. B.; de Resende, M. A.; Martins, C. V. B.; de Fátima, A. Schiff bases: A short review of their antimicrobial activities. *J. Adv. Res.* **2011**, *2*, 1–8.
- Login, C. C.; Báldea, I.; Tipericiu, B.; Benedec, D.; Vodnar, D. C.; Decea, N.; Suci, Ş. A novel thiazolyl Schiff base: Antibacterial and antifungal effects and in vitro oxidative stress modulation on human endothelial cells. *Oxid. Med. Cell. Longev.* **2019**, *2019*, 1607903.
- Murugaiyan, M.; Mani, S. P.; Sithique, M. A. Zinc(ii) centered biologically active novel N,N,O donor tridentate water-soluble hydrazide-based O-carboxymethyl chitosan Schiff base metal complexes: synthesis and characterisation. *New J Chem* **2019**, *43*, 9540–9554.
- Gwaram, N. S.; Ali, H. M.; Abdulla, M. A.; Buckle, M. J. C.; Sukumaran, S. D.; Chung, L. Y.; Othman, R.; Alhadi, A. A.; Yehye, W. A.; Hadi, A. H. A.; Hassandarvish, P.; Khaledi, H.; Abdelwahab, S. I. Synthesis, characterization, X-ray crystallography, acetyl cholinesterase inhibition and antioxidant activities of some novel ketone derivatives of gallic hydrazide-derived Schiff bases. *Molecules* **2012**, *17*, 2408–2427.
- Devi, J.; Pachwania, S. Synthesis, characterization, in vitro antioxidant and antimicrobial activities of diorganotin(IV) complexes derived from hydrazide Schiff base ligands. *Phosphorus Sulfur Silicon Relat. Elem.* **2021**, *196*, 1049–1060.
- Li, L.; Li, Z.; Wang, K.; Liu, Y.; Li, Y.; Wang, Q. Synthesis and antiviral, insecticidal, and fungicidal activities of Schiff's bases containing alkylimine, oxime or hydrazine moiety. *Bioorg. Med. Chem.* **2016**, *24*, 474–483.
- Liang, C.; Xia, J.; Lei, D.; Li, X.; Yao, Q.; Gao, J. Synthesis, in vitro and in vivo antitumor activity of symmetrical bis-Schiff base derivatives of isatin. *Eur. J. Med. Chem.* **2014**, *74*, 742–750.
- Alafeefy, A. M.; Bakht, M. A.; Ganaie, M. A.; Ansarie, M. N.; El-Sayed, N. N.; Awaad, A. S. Synthesis, analgesic, anti-inflammatory and anti-ulcerogenic activities of certain novel Schiff's bases as fenamate isosteres. *Bioorg. Med. Chem. Lett.* **2015**, *25*, 179–183.
- Abood, H. S.; Ramadhan, U. H.; Hamza, H. Synthesis and Anti-Inflammatory Activity Study of Schiff Bases Complexes. *Biochem. Cell. Arch.* **2020**, *20*, 5627–5631. https://www.researchgate.net/publication/346728834_synthesis_and_anti-inflammatory_activity_study_of_schiff_bases_complexes (accessed April 10, 2022).
- Mukherjee, S.; Pal, C. K.; Kotakonda, M.; Joshi, M.; Shit, M.; Ghosh, P.; Choudhury, A. R.; Biswas, B. Solvent induced distortion in a square planar copper(II) complex containing an azo-functionalized Schiff base: Synthesis, crystal structure, in-vitro fungicidal and anti-proliferative, and catecholase activity. *J. Mol. Struct.* **2021**, *1245*, 131057.
- Dey, D.; Kaur, G.; Patra, M.; Choudhury, A. R.; Kole, N.; Biswas, B. A perfectly linear trinuclear zinc-Schiff base complex: Synthesis, luminescence property and photocatalytic activity of zinc oxide nanoparticle. *Inorganica Chim. Acta* **2014**, *421*, 335–341.
- Gupta, K. C.; Sutar, A. K. Catalytic activities of Schiff base transition metal complexes. *Coord. Chem. Rev.* **2008**, *252*, 1420–1450.
- Assey, G. E.; Mgohamwende, R. A review of Titanium, Vanadium and Chromium transition metal Schiff base complexes with biological and catalytic activities. *Pharm. Pharmacol. Int. J.* **2020**, *8*, 136–146.
- Bermejo, M. R.; Carballido, R.; Fernández-García, M. I.; González-Noya, A. M.; González-Riopadre, G.; Maneiro, M.; Rodríguez-Silva, L. Synthesis, characterization, and catalytic studies of Mn(III)-Schiff base-dicyanamide complexes: Checking the rhombicity effect in peroxidase studies. *J. Chem.* **2017**, *2017*, 1–10.
- Kumar Mudi, P.; Das, A.; Mahata, N.; Biswas, B. Head-to-Tail interlocking aromatic rings of a hydrazine functionalized Schiff base for the development of Nano-aggregates with blue emission: Structural and spectroscopic characteristics. *J. Mol. Liq.* **2021**, *340*, 117193.
- Afzal, H. R.; Khan, N. U. H.; Sultana, K.; Mobashar, A.; Lareb, A.; Khan, A.; Gull, A.; Afzaal, H.; Khan, M. T.; Rizwan, M.; Imran, M. Schiff bases of pioglitazone provide better antidiabetic and potent antioxidant effect in a streptozotocin-nicotinamide-induced diabetic rodent model. *ACS Omega* **2021**, *6*, 4470–4479.
- Szklarzewicz, J.; Jurowska, A.; Hodorowicz, M.; Kazek, G.; Mordyl, B.; Menaszek, E.; Sapa, J. Characterization and antidiabetic activity of salicylhydrazone Schiff base vanadium(IV) and (V) complexes. *Transit. Met. Chem.* **2021**, *46*, 201–217.
- CrystalClear 2.0, Rigaku Corporation: Tokyo, Japan.
- Dolomanov, O. V.; Bourhis, L. J.; Gildea, R. J.; Howard, J. A. K.; Puschmann, H. OLEX2: a complete structure solution, refinement and analysis program. *J. Appl. Crystallogr.* **2009**, *42*, 339–341.
- Sheldrick, G. M. A short history of SHELX. *Acta Crystallogr. A* **2008**, *64*, 112–122.
- Spackman, M. A.; Jayatilaka, D. Hirshfeld surface analysis. *CrystrEngComm* **2009**, *11*, 19–32.
- McKinnon, J. J.; Jayatilaka, D.; Spackman, M. A. Towards quantitative analysis of intermolecular interactions with Hirshfeld surfaces. *Chem. Commun. (Camb.)* **2007**, 3814–3816.
- Mackenzie, C. F.; Spackman, P. R.; Jayatilaka, D.; Spackman, M. A. CrystalExplorer model energies and energy frameworks: extension to metal coordination compounds, organic salts, solvates and open-shell systems. *IUCr* **2017**, *4*, 575–587.
- Sahu, R.; Kundu, P.; Sethi, A. In vitro antioxidant activity and enzyme inhibition properties of wheat whole grain, bran and flour defatted with hexane and supercritical fluid extraction. *Lebenson. Wiss. Technol.* **2021**, *146*, 111376.
- Roberts, J. D.; Caserio, M. C. *Basic principles of organic chemistry*; 2nd ed.; Benjamin-Cummings Publishing Co., Subs. of Addison Wesley Longman: Reading, PA, 1977.

- [41]. Zugenmaier, P. Review of crystalline structures of some selected homologous series of rod-like molecules capable of forming liquid crystalline phases. *Int. J. Mol. Sci.* **2011**, *12*, 7360–7400.
- [42]. Saeed, S.; Rashid, N.; Mohamed, S. K. Synthesis and X-ray crystallography of N,N'-di(2-hydroxybenzylidene)hydrazine. *Eur. J. Chem.* **2017**, *8*, 15–17.
- [43]. Hanefeld, M. Cardiovascular benefits and safety profile of acarbose therapy in prediabetes and established type 2 diabetes. *Cardiovasc. Diabetol.* **2007**, *6*, 20.
- [44]. Rosak, C.; Mertes, G. Critical evaluation of the role of acarbose in the treatment of diabetes: patient considerations. *Diabetes Metab. Syndr. Obes.* **2012**, *5*, 357–367.
- [45]. DiNicolantonio, J. J.; Bhutani, J.; O'Keefe, J. H. Acarbose: safe and effective for lowering postprandial hyperglycaemia and improving cardiovascular outcomes. *Open Heart* **2015**, *2*, e000327.



Copyright © 2022 by Authors. This work is published and licensed by Atlanta Publishing House LLC, Atlanta, GA, USA. The full terms of this license are available at <http://www.eurjchem.com/index.php/eurjchem/pages/view/terms> and incorporate the Creative Commons Attribution-Non Commercial (CC BY NC) (International, v4.0) License (<http://creativecommons.org/licenses/by-nc/4.0>). By accessing the work, you hereby accept the Terms. This is an open access article distributed under the terms and conditions of the CC BY NC License, which permits unrestricted non-commercial use, distribution, and reproduction in any medium, provided the original work is properly cited without any further permission from Atlanta Publishing House LLC (European Journal of Chemistry). No use, distribution or reproduction is permitted which does not comply with these terms. Permissions for commercial use of this work beyond the scope of the License (<http://www.eurjchem.com/index.php/eurjchem/pages/view/terms>) are administered by Atlanta Publishing House LLC (European Journal of Chemistry).